Order development in polymer-clay nanocomposites: from aqueous gels to multilayered films

Eduard A. Stefanescu,[1] Cristina Stefanescu,[2] William H. Daly [2] and Ioan I. Negulescu [2]

[1]Department of Chemical & Life Science Engineering, Virginia Commonwealth University, Richmond, VA 23284, USA, tel: 804-827-7000 x 456, fax: 804-828-3846, e-mail: eastefanescu@vcu.edu

[2]Department of Chemistry, Louisiana State University, Baton Rouge, LA 70803, USA

ABSTRACT

The aim of the present contribution is to correlate the extent of internal orientation developed in salt containing montmorillonite (CNA)-poly(ethylene oxide) dispersions subjected to shear and elongational deformations with the high degrees of anisotropy observed in multilayered films prepared from the tested precursor gels. Entropic changes indicate that the strength of the transient network present in each gel affects the orientational ability of clay particles and polymer chains. The shear orientation of a polymer-clay network in solution combined with simultaneous solvent evaporation leads to supramolecular multilayer formation in the solid film. In the films, the polymer-covered clay platelets are highly structured and oriented preferentially with the surface parallel to the plane of the film. The overall concentration of the polymer-clay dispersions influences decisively the final layered texture of the solid films, as seen by SEM.

Keywords: PEO, clay, nanocomposite, rheology, order

BACKGROUND

The interaction of the polymer with the particle and the particle orientation in an aqueous precursor phase may lead to a variety of ordered composite materials in the bulk or film.*[1, 2]* Disk-like clay particles promote supramolecular organization*[2, 3]* similar to other systems such as liquid crystalline polymers*[4]* or surfactants*[5]*. Typically the rheological behavior of nanocomposite gels is studied to identify the relationship existing between gels composition and their performance under shear, as well as to observe the variation of viscosity, storage and loss moduli as a function of several parameters in the nanocomposite dispersions. Identifying these properties and relationships is critical for achieving a fundamental understanding of materials processability. Furthermore, rheological studies correlated with mechanical studies on films may offer valuable information regarding the relationships existent between the strength of the polymer-clay network in the precursor dispersions and the structure and properties of the resultant multilayered nanocomposite films prepared from such dispersions.

EXPERIMENTAL

Montmorillonite clay, cloisite Na^+ (CNA), (a gift from Southern Clay Products) was used as received. PEO with a molecular mass of 1000 kg/mol (Mw/Mn=1.5) was used as received from Polysciences Inc. The dispersion pH was controlled by addition of NaOH (pH ≈ 9) to ensure a good stability of the clay. One set of exfoliated gels, with compositions of 6% CNA and 4% PEO (90% water), and containing NaCl salt, was produced. The amount of NaCl was adjusted in the gels to ensure a ratio of $EO/Na^+=8$ (EO are ethylene oxide groups). Another set of exfoliated dispersions containing 3% CNA and 2% PEO (95% water) was also prepared. This set of dispersions incorporates NaCl electrolyte, just like the CNA6%-PEO4% gels, but in a concentration of $5.5*10^{-5}$ M. Only the gels with a composition of 6% CNA and 4% PEO were subjected to elongational flow.

Multilayered films were prepared by manually spreading the hydrogels on glass slides with a spatula every 2 hours. Overnight, samples were dried in desiccators. On average, 5 layers were spread every day. Films with the same spreading direction were dried layer by layer one on top of another until a total thickness of about 0.25 mm was obtained for the multilayered film. By evaporating the water in the drying process all films resulted with compositions of 40% polymer and 60% clay.

RESULTS AND DISCUSSION

1. Rheology of nanocomposite gels

When passing a material through a hyperbolic convergent die in an elongational rheometer, high degrees of order are induced in the material, and the entropy changes, indicative of orientation, can be calculated. *[6-8]* The main advantage of the hyperbolic convergent die over the cylindrical die is that the elongational strain rate generated by the first is constant throughout the core of the material. *[9]* The Hencky strain, ε_H, of the hyperbolic convergent die is defined as the natural logarithm of the area reduction of the die:

$$\varepsilon_H = 2ln\frac{r_0}{r_e} \quad (1)$$

where r_0 and r_e are the inlet and outlet radii of the die respectively.*[7]* As demonstrated by Collier et al,*[8]* the enthalpy change per unit volume, ΔH, necessary for calculating the variation of entropy, can be expressed as:

$$\Delta H = -\varepsilon_H \dot{\varepsilon}(\eta_{ef} - 3\eta_s) \quad (2)$$

In equation (2) $\dot{\varepsilon}$ is the elongational strain rate, η_{ef} is the effective elongational viscosity, and η_s represents the shear viscosity of the fluid, obtained from shear rheology measurements. Numerical simulations showed that η_{ef} provides a good approximation of η_e ,*[10]* for which reason we consider $\eta_e = \eta_{ef}$. The term η_e represents the elongational viscosity as given by the elongational rheometer. Combining the Gibbs free energy relation, $\Delta F=\Delta H-T\Delta S$, with equation 2, the entropy change, ΔS, indicating the degree of orientation developed in the fluid dispersion can be written as:

$$\Delta S = \frac{-\varepsilon_H \dot{\varepsilon}(\eta_e - 3\eta_s)}{T} \quad (3)$$

where T is the temperature expressed in Kelvin. A more detailed methodology for calculating the entropy changes from elongational flow processes is described elsewhere. *[8, 10]*

From the shear- and elongational-rheology data (not shown here) *[9]* the entropy changes of the CNA6%-PEO4% nanocomposite gels were calculated and are presented in figure 1. It can be observed that the degree of orientation developed in the gel subjected to elongational flow increases with the increase of the elongational strain applied in the process. The entropy change also varies with the Hencky strain of the hyperbolic die used in the elongational-flow process, where an increase in the Hencky strain results in a higher variation of the calculated entropy of the material. CNA3%-PEO2% dispersions could not be subjected to elongational flow measurements because they were not self-supporting gels.

From previous studies we know that polymers that are long enough to form inter-particle bridges promote formation of a reversible polymer-clay network that dominates the rheological response of the system.*[11]* At rest, all polymer-clay samples consist of a network between randomly oriented clay platelets and PEO chains with polymer chains acting as dynamic cross-links between the platelets. Under shear the clay platelets orient along the flow direction with the surface normal to vorticity direction.*[12]*

Shear viscosity experiments for the CNA3%-PEO2% dispersions are presented in figure 2a in an attempt to correlate the shear orientation with the final orientation in the dried films. A remarkable feature in figure 2a is the occurrence of a transition in the system at shear rates higher

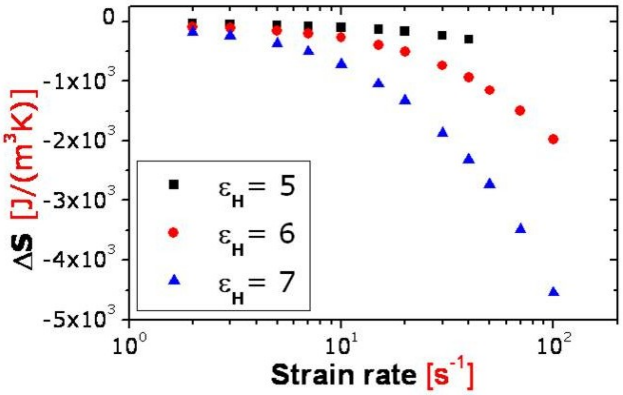

Figure 1. Entropy change from rheology for the NaCl-containing CNA6%-PEO4% gel (90% water).

than 10^1 s^{-1}. This feature was not observed for the CNA6%-PEO4% gels subjected to shear deformations (not shown here). The transition is temperature dependent where an increase in temperature shifts the transition peak to higher shear rates. In addition to shifting the transitions' shear rates, temperature has also an effect on the magnitude of the transition, where higher temperatures result in larger transitions. At lower shear rates, before reaching the transition domain, there is a near linear relationship between the log(η) and log(dγ/dt). This indicates that over the shear rate dependent region the solutions are power law fluids that exhibit shear thinning behavior. The power law relation can be expressed as $\eta = m(d\gamma/dt)^{n-1}$, where η is the shear viscosity (Pa*s), *m* is the consistency index, dγ/dt ($d\gamma/dt=\dot{\gamma}$) is the shear rate (s^{-1}), and *n* is the power law index and has values comprised between 0 and 1. The power law index for all three curves in figure 2a was calculated to be *n* = 0.5(+/-0.03).

To verify the agreement and accuracy of the data, and to rule out any instrument artifacts that might have been present in the measurements at high shear rates, the curves from figure 2a were combined into a master curve presented in figure 2b. In this figure the curve at 25°C was used as a reference for shifting the other two shear viscosity curves. The shift factors, a_T, were determined based on a relation described by Young and Lovell: *[13]*

$$log\ a_T = log\ \omega_{ref} - log\ \omega \quad (4)$$

where a_T is the shift factor and represents the temperature dependence of the relaxation times, ω_{ref} and ω represent angular frequencies in the reference and non-reference curves. Combining the equivalence of ω with $\dot{\gamma}$, introduced by the extended Cox-Mertz rule,*[14-16]* with relation (4) the following equation was obtained:

$$log\ a_T = log\ \dot{\gamma}_{ref} - log\ \dot{\gamma} \quad (5)$$

where $\dot{\gamma}_{ref}$ and $\dot{\gamma}$ ($\dot{\gamma}=d\gamma/dt$) represent shear rate values for the reference and non-reference curves. Relation (5) was used to calculate the shift - factors discussed here. In this

NSTI-Nanotech 2009, www.nsti.org, ISBN 978-1-4398-1782-7 Vol. 1, 2009

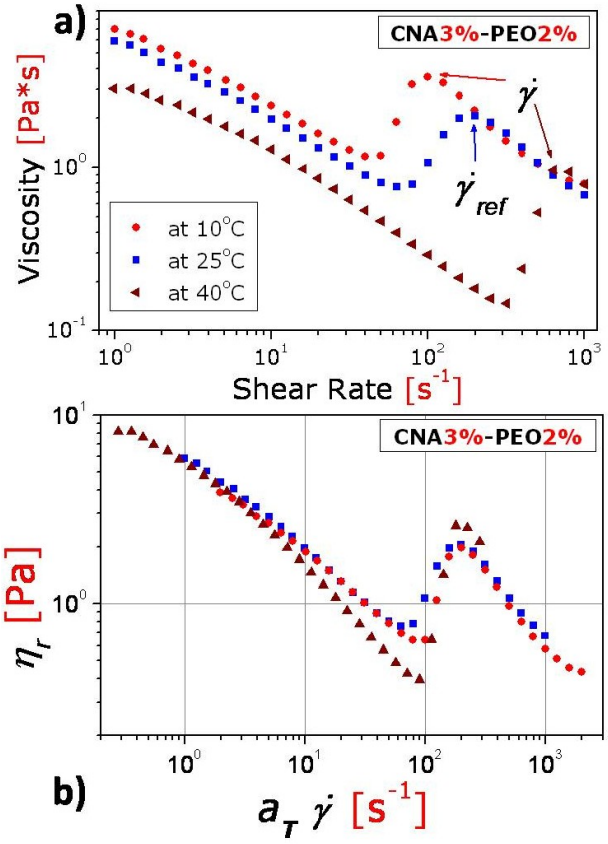

Figure 2. (a) Viscosity values as a function of shear rate for CNA3%-PEO2% nanocomposite gels; **(b)** Master curve obtained by superimposing the viscosity curves presented in **(a)**. The curve obtained at 25°C was used as a reference curve.

relation $\dot{\gamma}_{ref}$ and $\dot{\gamma}$ were chosen to be the shear rates of the reference and non-reference curves for which the viscosity of the transition peak was maximum (indicated by arrows in figure 2a). After finding the shift factors, the reduced viscosity was calculated using the relation described by Morisson: *[16]*

$$\eta_r = [\eta(T)^* T_{ref}{}^* \rho_{ref}]/[\, a_T{}^* T^* \rho] \qquad (6)$$

where η_r is the reduced viscosity, T_{ref} (K) is the polymer glass transition temperature, Tg(K), ρ_{ref} is the polymer density at Tg, T(K) is the reference temperature used for shifting the curves, and ρ is the density of the polymer solution at the shifting temperature. The PEO glass transition was considered Tg=207K,*[17]* ρ_{ref} = 1.1g/cm^3,*[14]* and ρ solution at 25°C (T=298K) was considered 1g/cm^3, since our gels contain 95% water. The resulted master curve shows a reasonably effective shifting technique, despite its simplicity. Not all the points of the shifted curves can overlap the reference curve, since the flow transitions have different magnitudes at different temperatures.

2. Multilayered nanocomposite films

Due to the ordering imposed in the shear spreading process the clay platelets are expected to be oriented with the surface parallel to the plane of the film, as indicated in the schematic shown in figure 3. In order to study the orientation of clay platelets in the multilayered film, SAXS

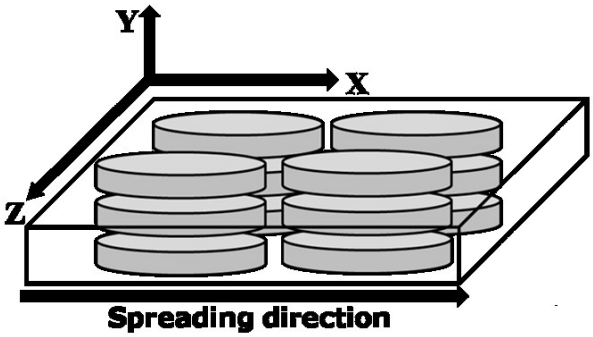

Figure 3. Schematic showing the idealized orientation of clay platelets in the film along with the definition of planes

measurements were carried out for two orientations of the sample with respect to the X-ray beam. The SAXS results, obtained from a multilayered film prepared using the CNA6%-PEO4% dispersion, are presented in figure 4. The isotropic SAXS pattern in the X-Z plane and the anisotropy observed in the X-Y plane confirms the orientation of the platelets to be with the surface parallel to the plane of the film. From the two-dimensional (2D) SAXS patterns the intensity as a function of q in the Z and Y directions was calculated (plot not shown here). The appearance of a peak at q ≈ 0.36Å^{-1} was correlated with d- spacing ($d_{SAXS}=2\pi/q$) in the order of 17.5Å that was attributed to the distance between stacked clay platelets. Small angle neutron scattering (SANS) measurements (not shown here) obtained from the multilayered film prepared with the CNA3%-PEO2% indicated similar results. *[18]*

SEM measurements, taken from the edge of the layered films, were performed to examine the film morphology at the micrometer scale. Figure 5a presents the edge of the

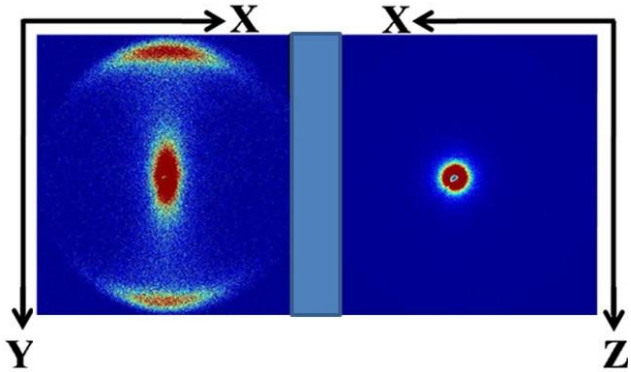

Figure 4. SAXS patterns resulted from the Z and Y directions for a nanocomposite film prepared from the CNA6%-PEO4% dispersion.

nanocomposite film prepared from the CNA3%-PEO2% dispersion, while figure 5b shows the edge of the film prepared from the CNA6%-PEO4% nanocomposite gel. Highly ordered and layered structures can be observed on the edge of both films while no layers are visible on the top surface (not shown here). As mentioned above, the aqueous CAN – PEO solutions can be described as interconnected

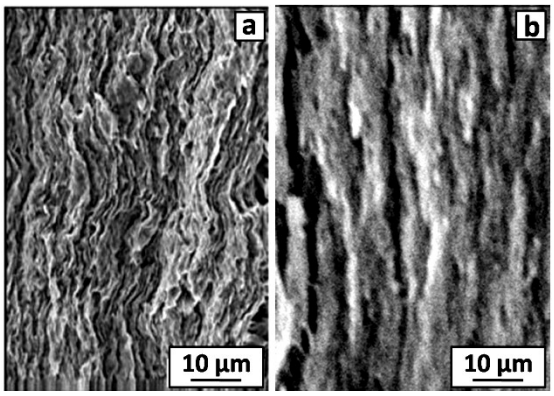

Figure 5. SEM micrographs obtained from the edge of the films prepared from: (a) CNA3%-PEO2% dispersion; (b) CNA6%-PEO4% dispersion. The vertical axis in the micrographs represents the spreading direction.

networks. When the sample is shear-oriented and the solvent evaporates simultaneously, the network collapses leading to layered film structures that can be observed on several length scales. The layered texture observed for the film prepared from the CNA3%-PEO2% dispersion is not uniform and is calculated to have an average dimension of 60–70 nm per layer. The number of multilayers can only be estimated since one single spread layer produces multiple layers on large length scales. *[18, 19]* On the other hand, for the film prepared from the CNA6%-PEO4% gel the multilayers are observed to group together in bundles of layers with a thickness of around 3 – 5 µm.

These structural differences are attributed to differences in the viscosity and network strength of the precursor gels used to prepare the multilayered films. As the viscosity and storage moduli of the gels increase, when the concentration of the solid material (clay + polymer) is increased, the internal CNA-PEO networks exhibit an increased resistance to the mechanical deformation imposed by the blade during shear spreading, leading to the formation of thicker bundles of multilayers.

CONCLUSION

We have studied the influence of composition on the structure and properties of PEO-montmorillonite dispersions and films and have found that the strength of the network and the viscosity in the gels increase significantly when the concentration of the solid material is varied, affecting the final structure of the multilayered films. Calculating the entropy changes developed during elongational flow can help identifying those gels that exhibit the highest degrees of orientation in the process. Since the structure and properties of polymer/clay films are strongly dependent on the structure of precursor dispersion/gels, changing key parameters in the gels can provide a useful route to obtaining highly anisotropic films with improved ionic conductivities and mechanical properties.

REFERENCES

[1] R. A. Vaia, E. P. Gianellis, *MRS Bulletin* **2001**, *62*, 394.
[2] G. Schmidt, M. M. Malwitz, *Current Opinion in Colloid & Interface Science* **2003**, *8*, 103.
[3] J. C. P. Gabriel, F. Camerel, B. J. Lemaire, H. Desvaux, P. Davidson, P. Batail, *Nature* **2001**, *413*, 504.
[4] G. Schmidt, S. Muller, C. Schmidt, W. Richtering, *Rheologica Acta* **1999**, *38*, 486.
[5] G. Schmidt, S. Muller, P. Lindner, C. Schmidt, W. Richtering, *Journal of Physical Chemistry B* **1998**, *102*, 507.
[6] J. R. Collier, *U.S. Patent 5,357,784* **1994**, *issued to LSU*.
[7] J. R. Collier, S. Petrovan, P. Patil, B. Collier, *Journal of Materials Science* **2005**, *40*, 5133.
[8] J. R. Collier, O. Romanoschi, S. Petrovan, *Journal of Applied Polymer Science* **1998**, *69*, 2357.
[9] E. A. Stefanescu, S. Petrovan, W. H. Daly, I. I. Negulescu, *Macromol. Mater. Eng.* **2008**, *293*, 303.
[10] K. Feigl, F. X. Tanner, B. J. Edwards, J. R. Collier, *J. Non-Newton. Fluid. Mech.* **2003**, *115*.
[11] G. Schmidt, A. I. Nakatani, C. C. Han, *Rheol Acta* **2002**, *41*, 45.
[12] G. Schmidt, A. I. Nakatani, P. D. Butler, C. C. Han, *Macromolecules* **2002**, *35*, 4725.
[13] R. J. Young, P. A. Lovell, *Introduction to Polymers*, CRC Press LLC, Boca Raton, FL 33431 **1991**.
[14] V. K. Daga, N. J. Wagner, *Rheol. Acta* **2006**, *45*, 813.
[15] J. M. Dealy, K. F. Wissbrun, *Melt Rheology and its Role in Plastics Processing; Theory and Applications*, Kluwer Academic Publishers, The Netherlands **1999**.
[16] F. A. Morrison, *Understanding Rheology*, Oxford University Press, Inc., New York, 10016 **2001**.
[17] J. M. G. Cowie, *Polymers: Chemistry & Physics of Modern Materials*, Nelson Thornes Ltd, Cheltenham, UK **1991**.
[18] E. A. Stefanescu, A. Dundigalla, V. Ferreiro, E. Loizou, L. Porcar, I. Negulescu, J. Garno, G. Schmidt, *Phys Chem Chem Phys* **2006**, *8*, 1739.
[19] E. A. Stefanescu, P. J. Schexnailder, A. Dundigalla, I. I. Negulescu, G. Schmidt, *Polymer* **2006**, *47*, 7339.